Supplementary Information

Photo-Induced Uncaging of a Specific Re(I) Organometallic Complex in Living Cells

Anna Leonidova,[a] Vanessa Pierroz,[a,b] Riccardo Rubbiani, [a] Yanjun Lan,[a] Anita G. Schmitz,[a] Andres Kaech,[c] Roland K. O. Sigel, [a] Stefano Ferrari[b] and Gilles Gasser[a,]*

[a] Department of Chemistry, University of Zurich, Winterthurerstrasse 190, CH-8057 Zurich, Switzerland; [b] Institute of Molecular Cancer Research, University of Zurich, Winterthurerstrasse 190, CH-8057 Zurich, Switzerland; [c] Center of Microscopy and Image Analysis, University of Zurich Winterthurerstrasse 190, CH-8057 Zurich, Switzerland

* Corresponding author: email: gilles.gasser@chem.uzh.ch; Fax : +41 44 635 68 03; Tel: +41 44 635 46 30; WWW: www.gassergroup.com.

Table of Contents

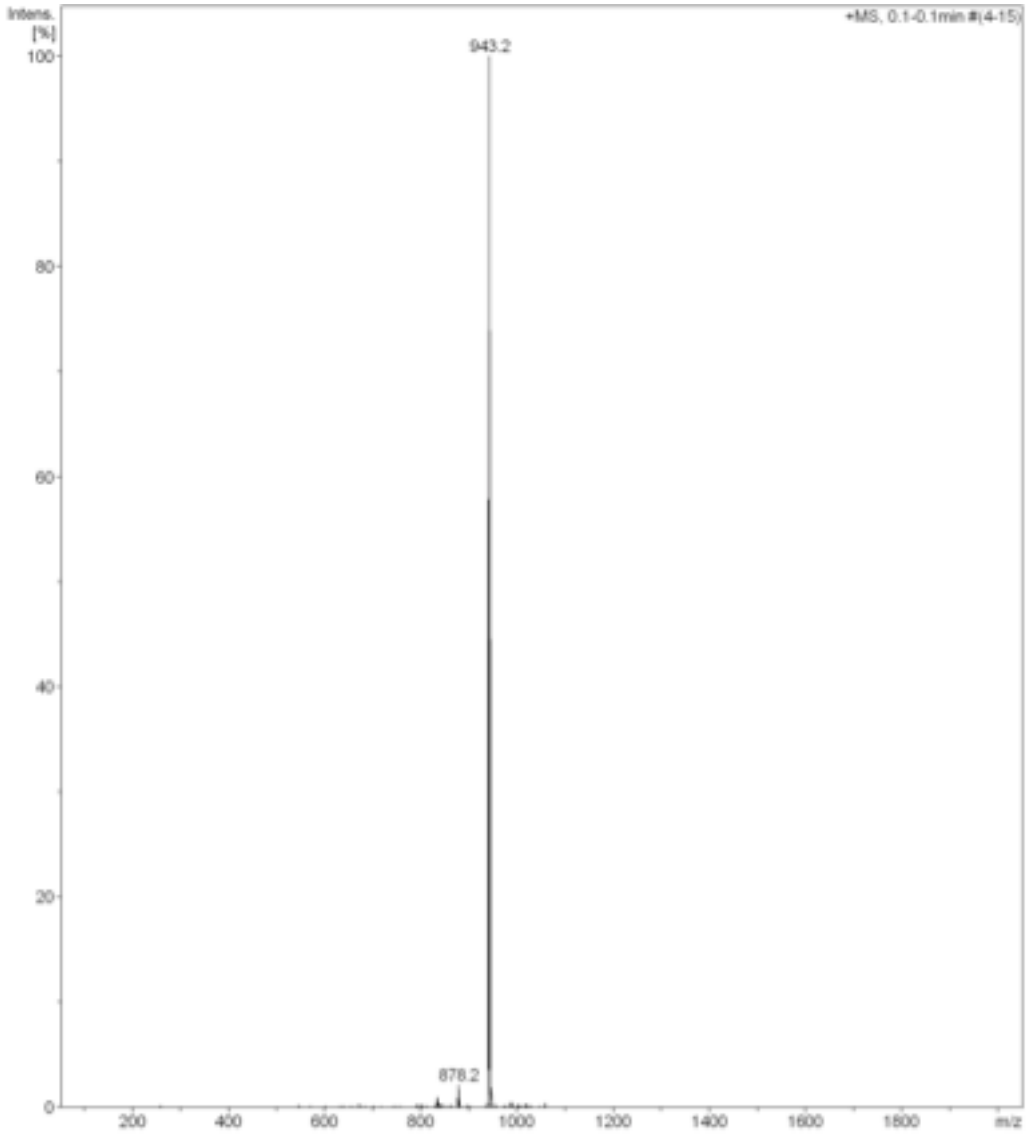

Figure S1. ESI-MS spectrum of **Re-PLPG**.

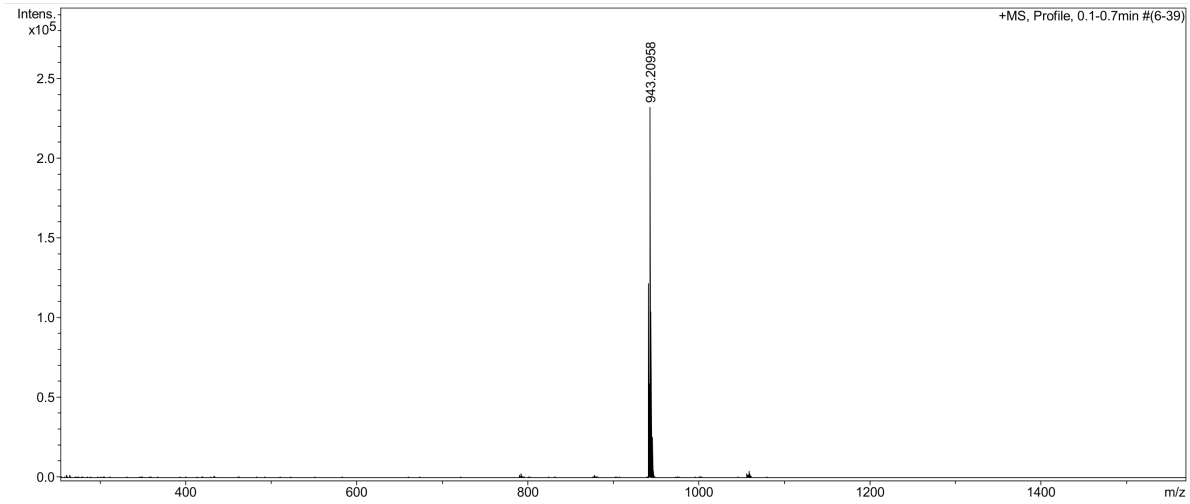

Figure S2. HR ESI-MS spectrum of **Re-PLPG**.

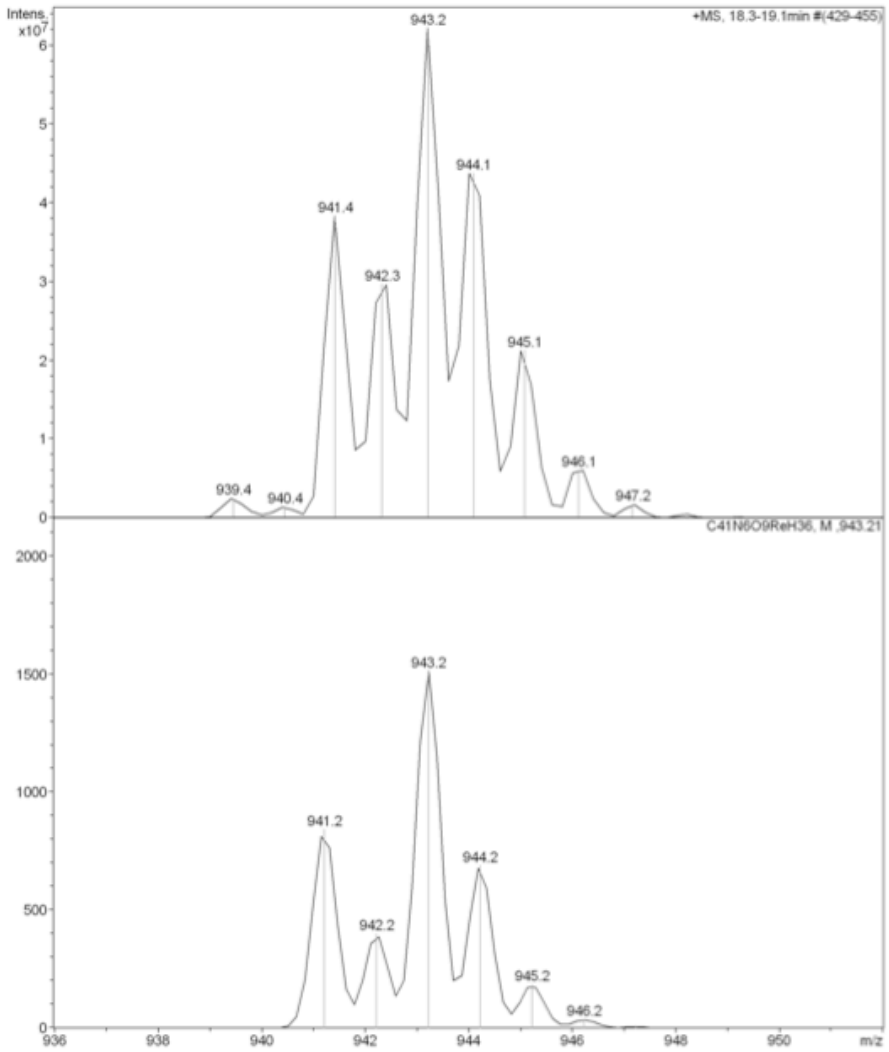

Figure S3. Recordered (above) and simulated (below) isotopic pattern of **Re-PLPG**.

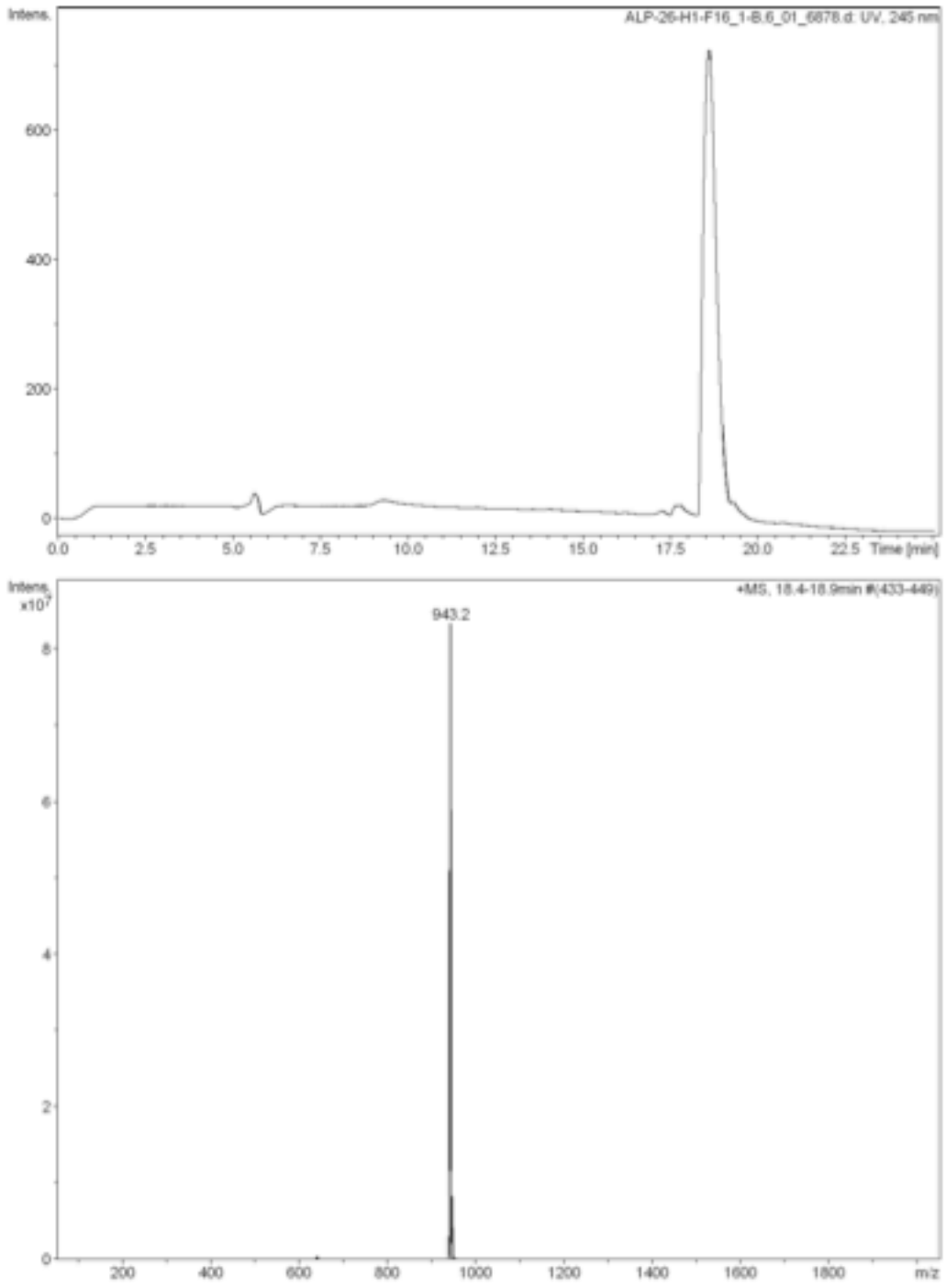

Figure S4. LC-MS spectrum of **Re-PLPG**.

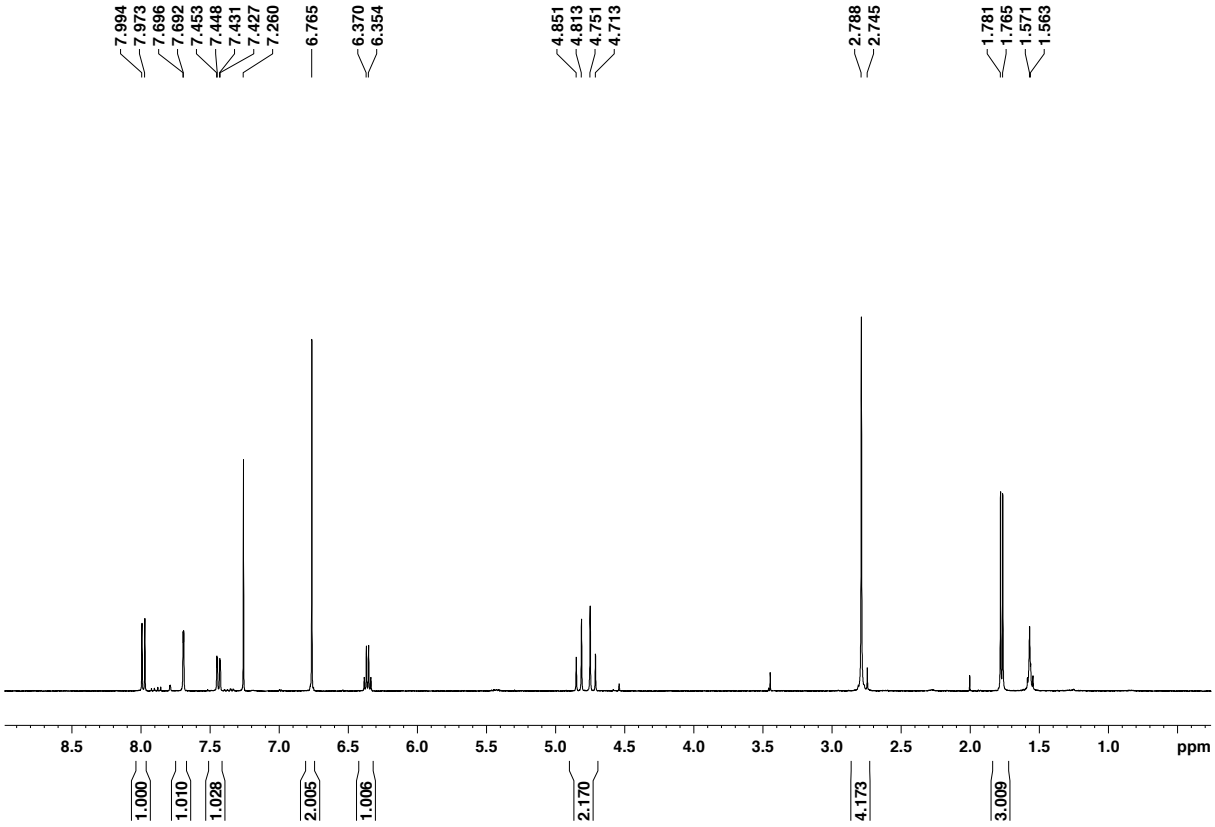

Figure S5. ^{1}H-NMR spectrum of **PLPG** in chloroform.

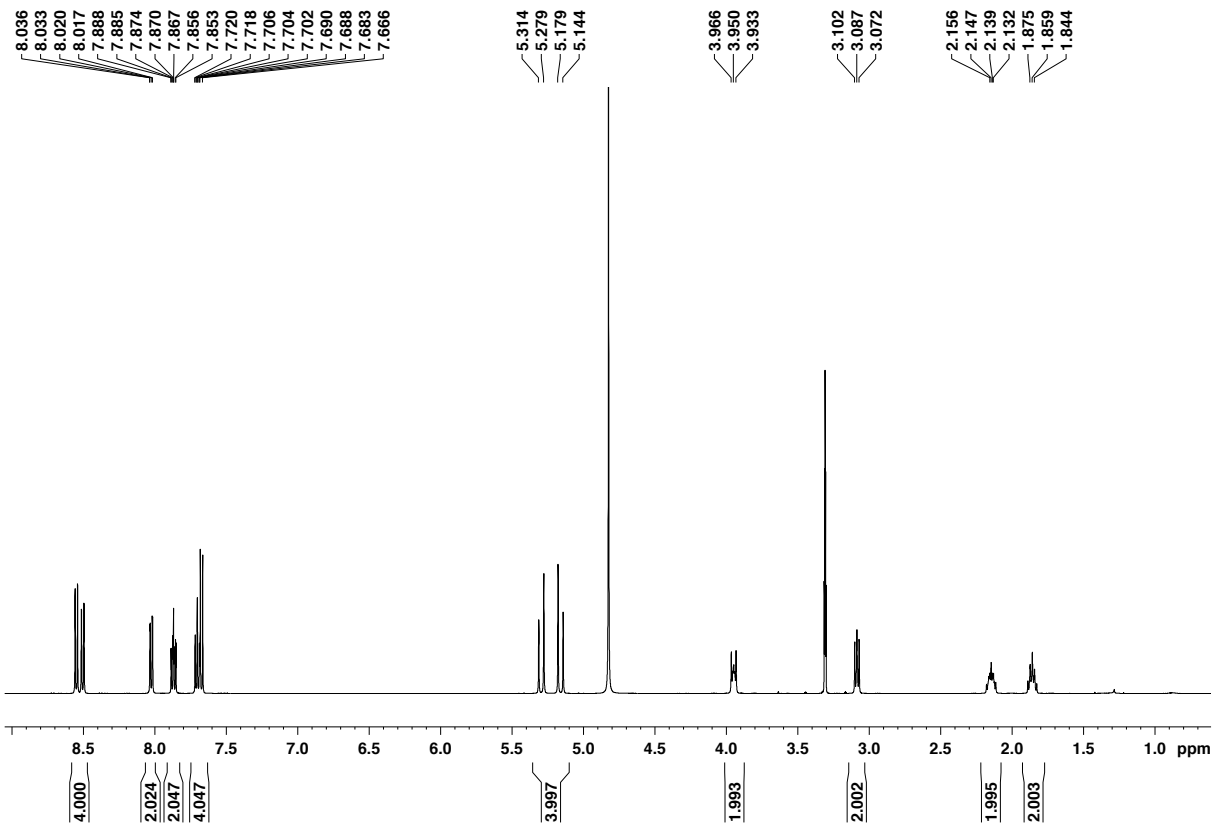

Figure S6. ^{1}H-NMR spectrum of **Re-NH$_2$** in MeOH.

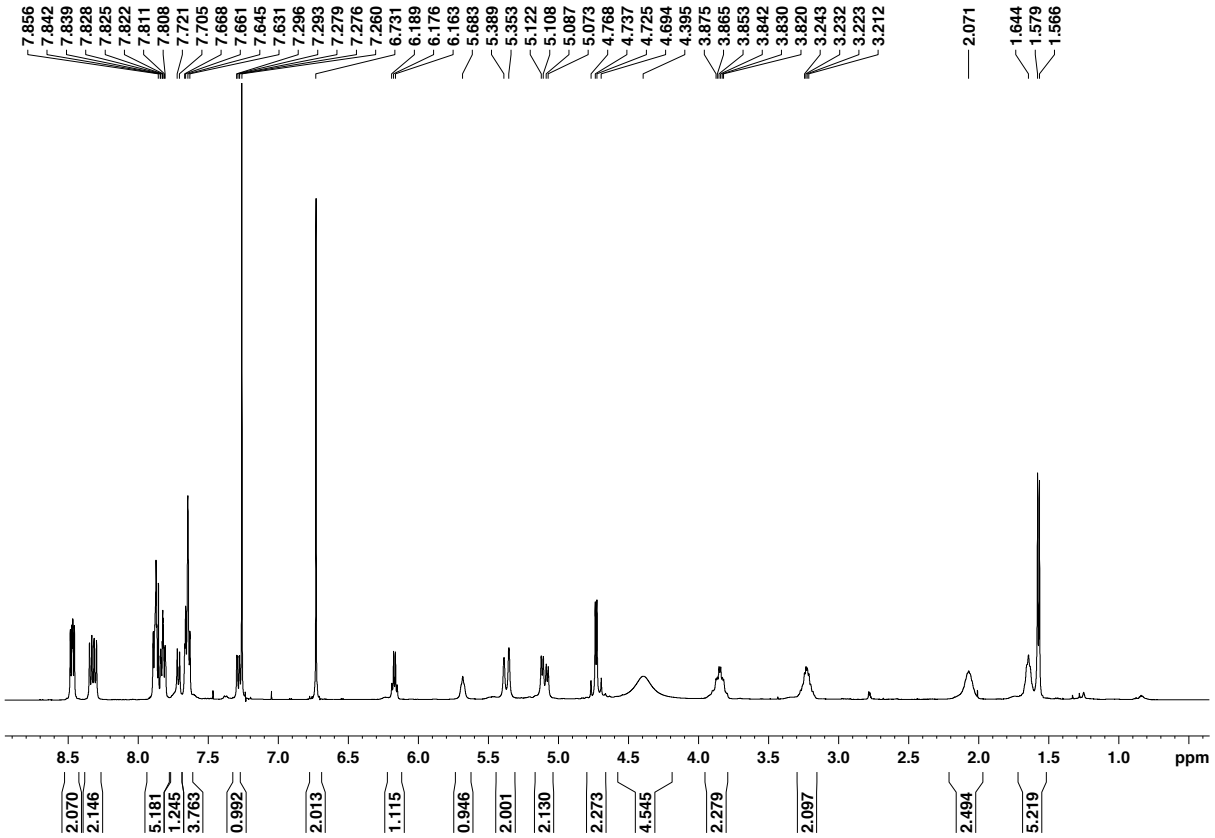

Figure S7. ^{1}H-NMR spectrum of **Re-PLPG** in chloroform.

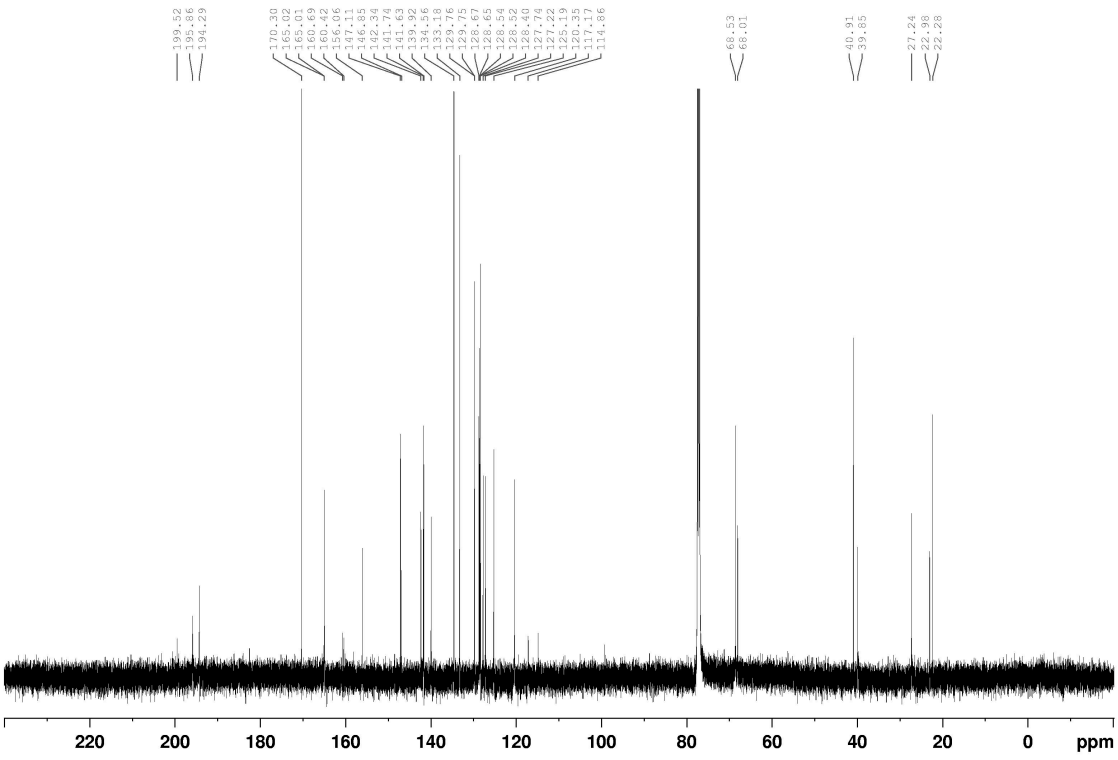

Figure S8. ^{13}C-NMR spectrum of **Re-PLPG** in chloroform.

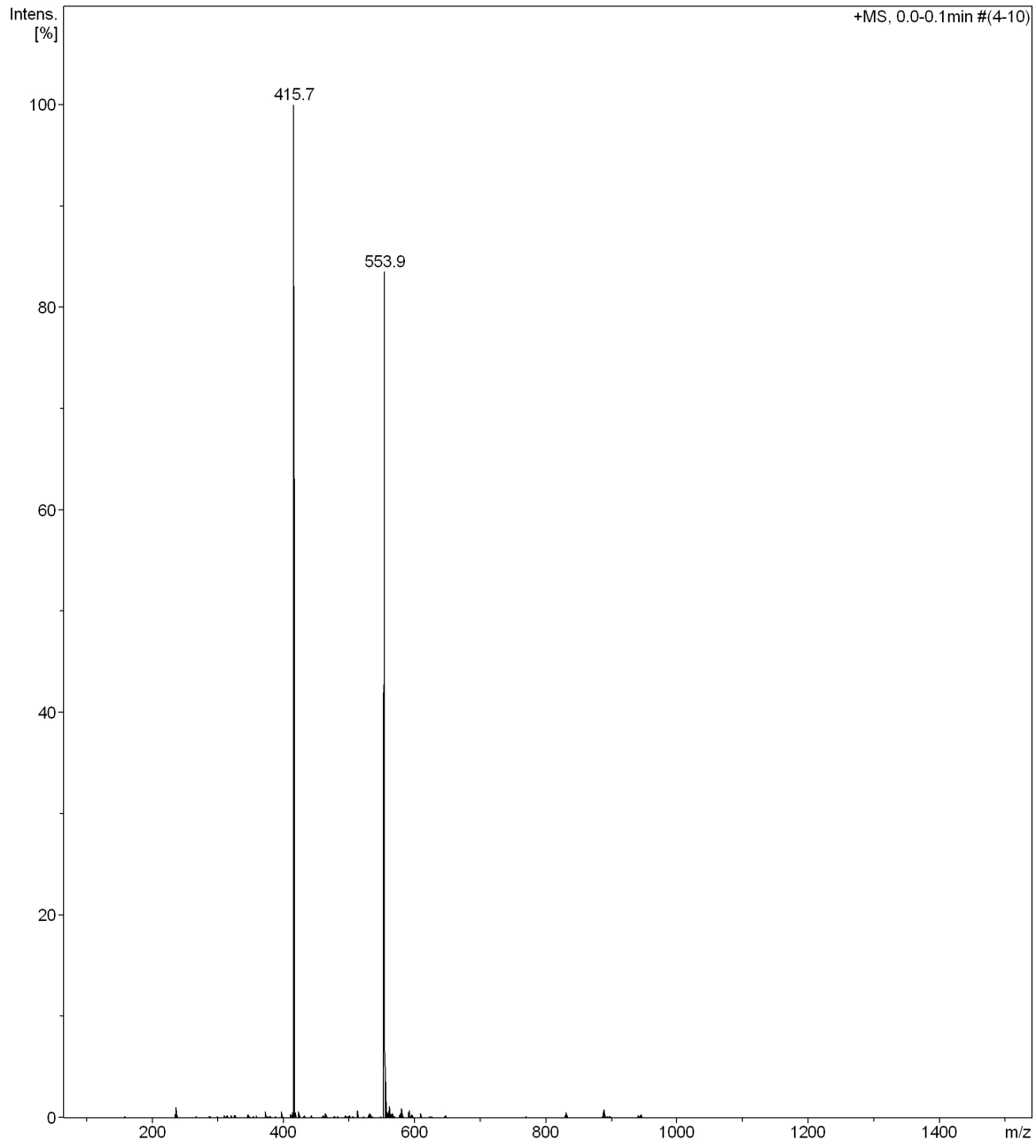

Figure S9. ESI-MS spectrum of **Re-PLPG-NLS**.

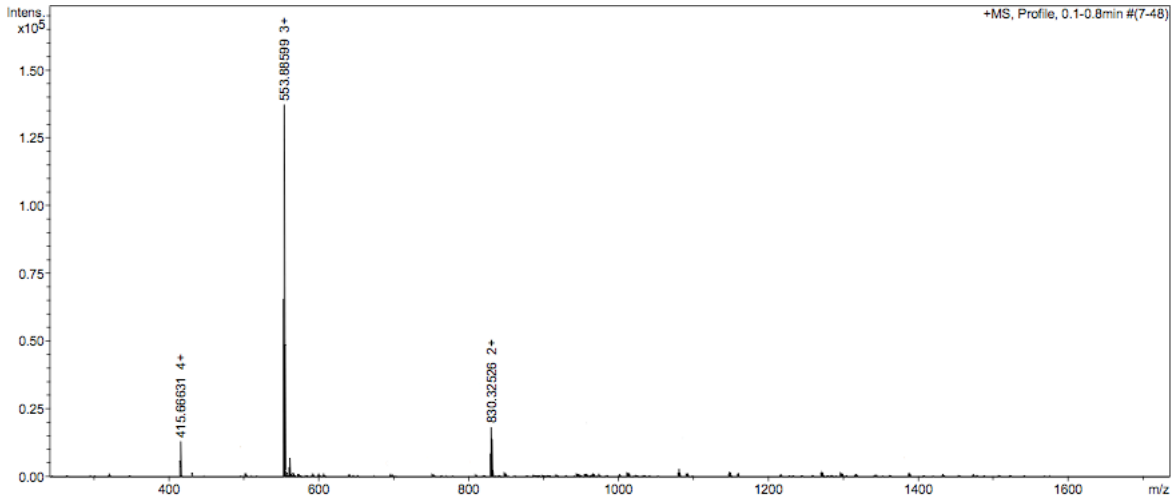

Figure S10. HR ESI-MS spectrum of **Re-PLPG-NLS**.

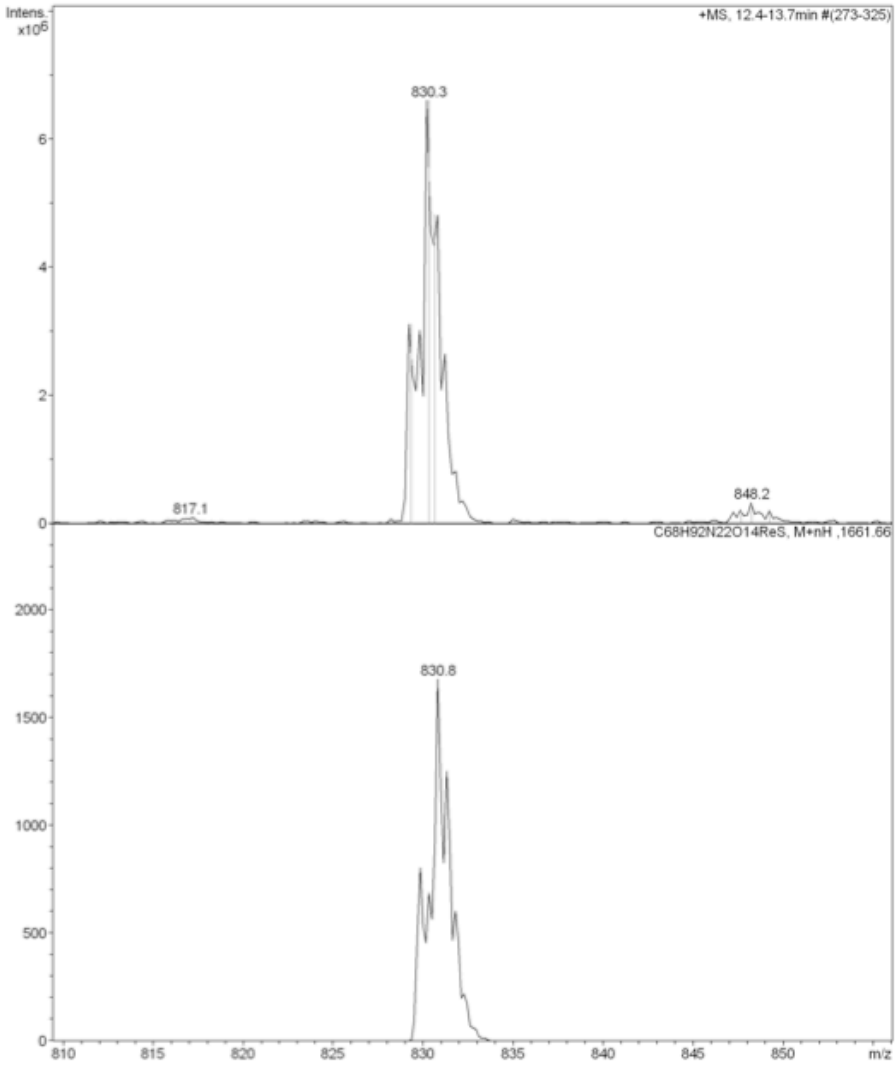

Figure S11. Recordered (above) and simulated (below) isotopic pattern of **Re-PLPG-NLS**.

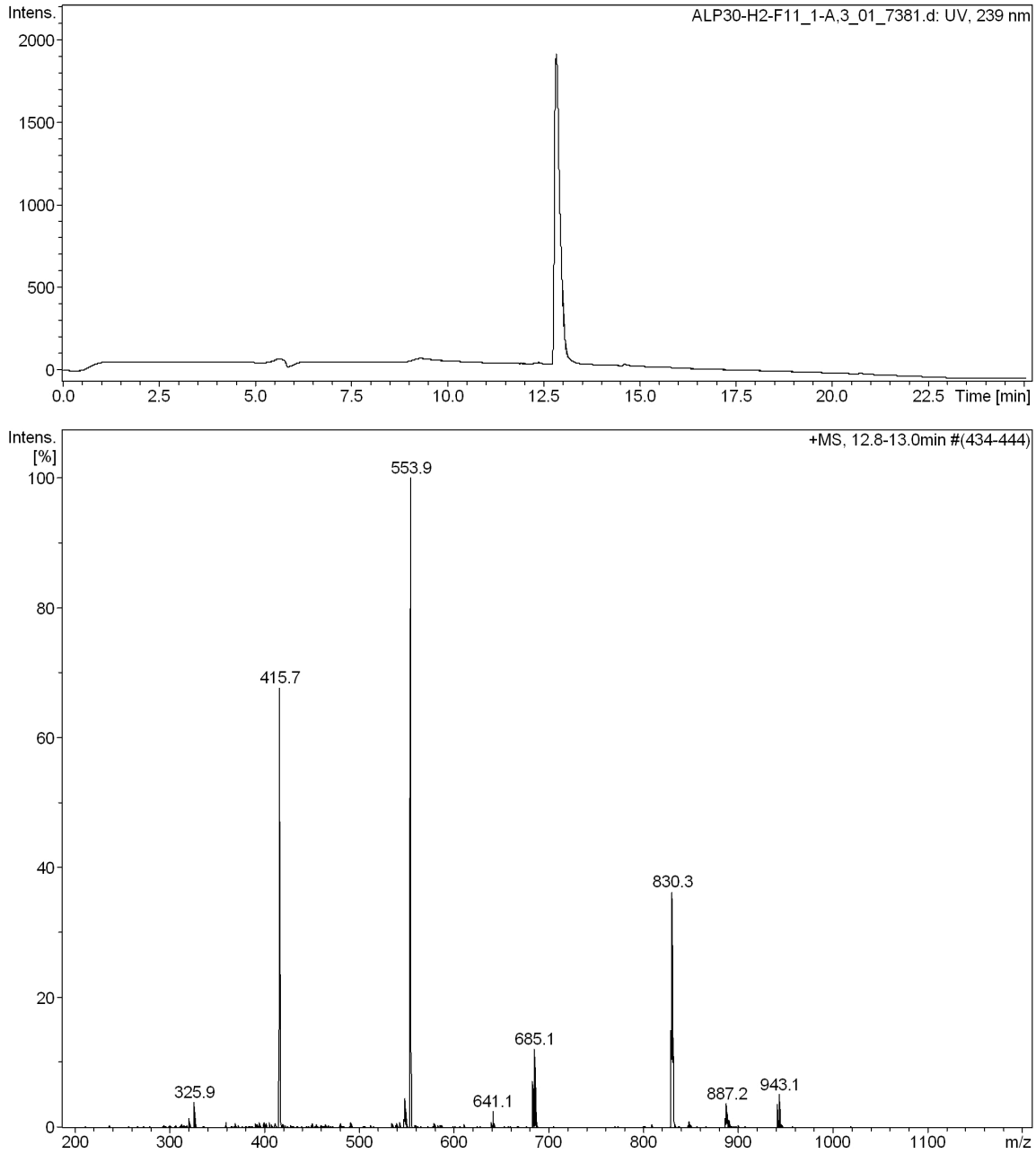

Figure S12. LC-MS spectrum of **Re-PLPG-NLS**.

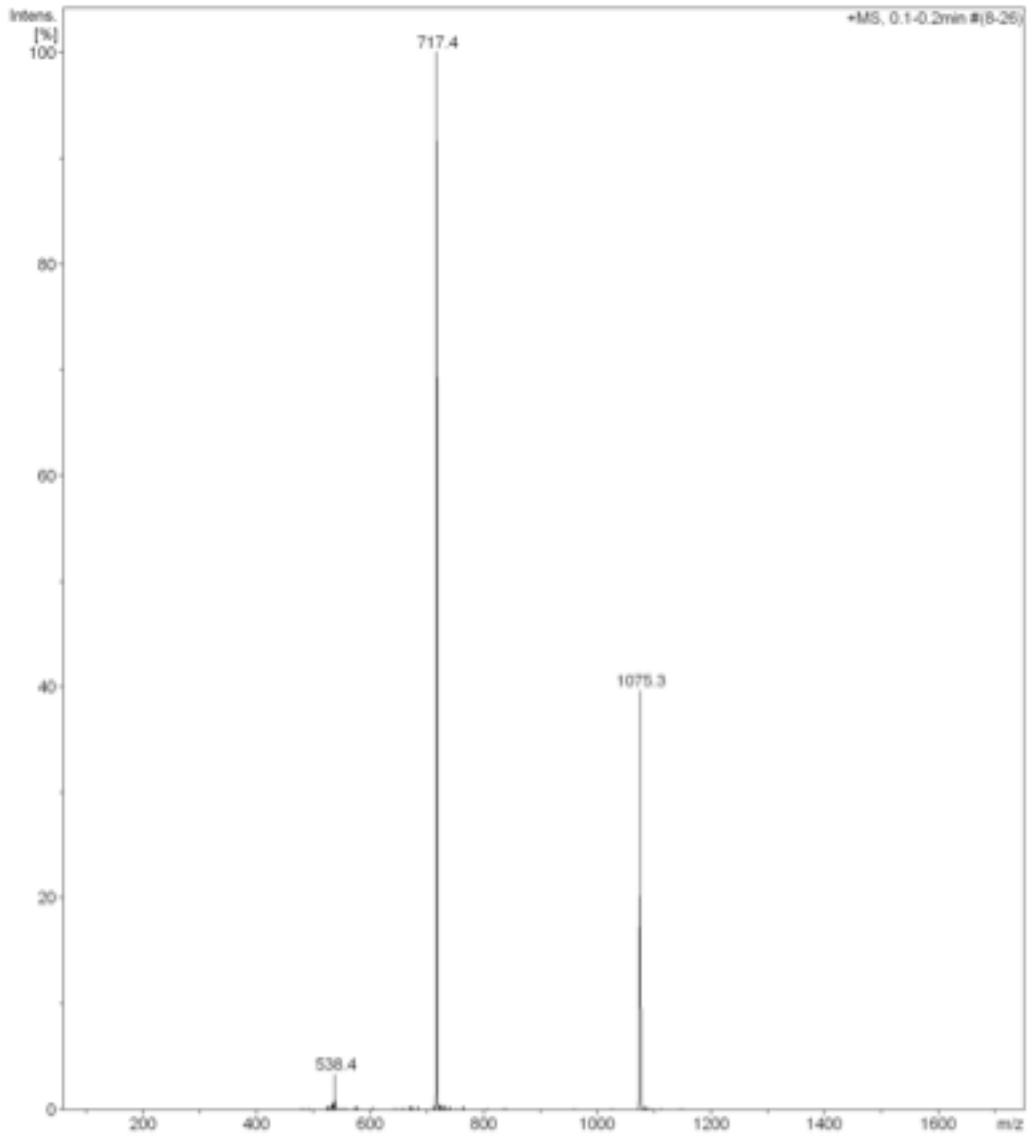

Figure S13. ESI-MS spectrum of **Re-PLPG-Bombesin**.

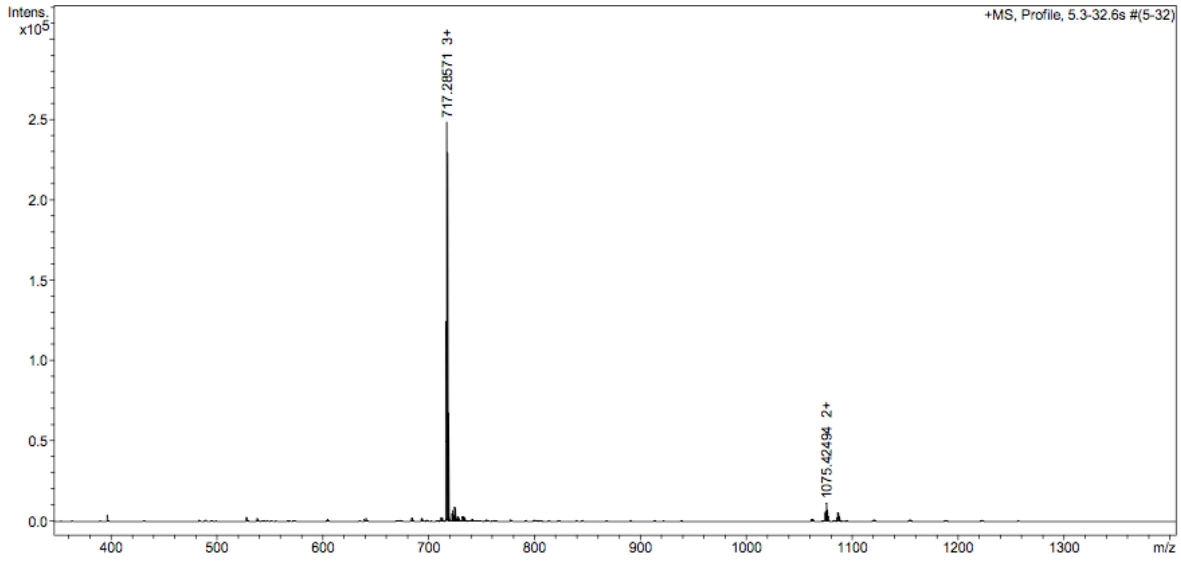

Figure S14. HR ESI-MS spectrum of **Re-PLPG-Bombesin**.

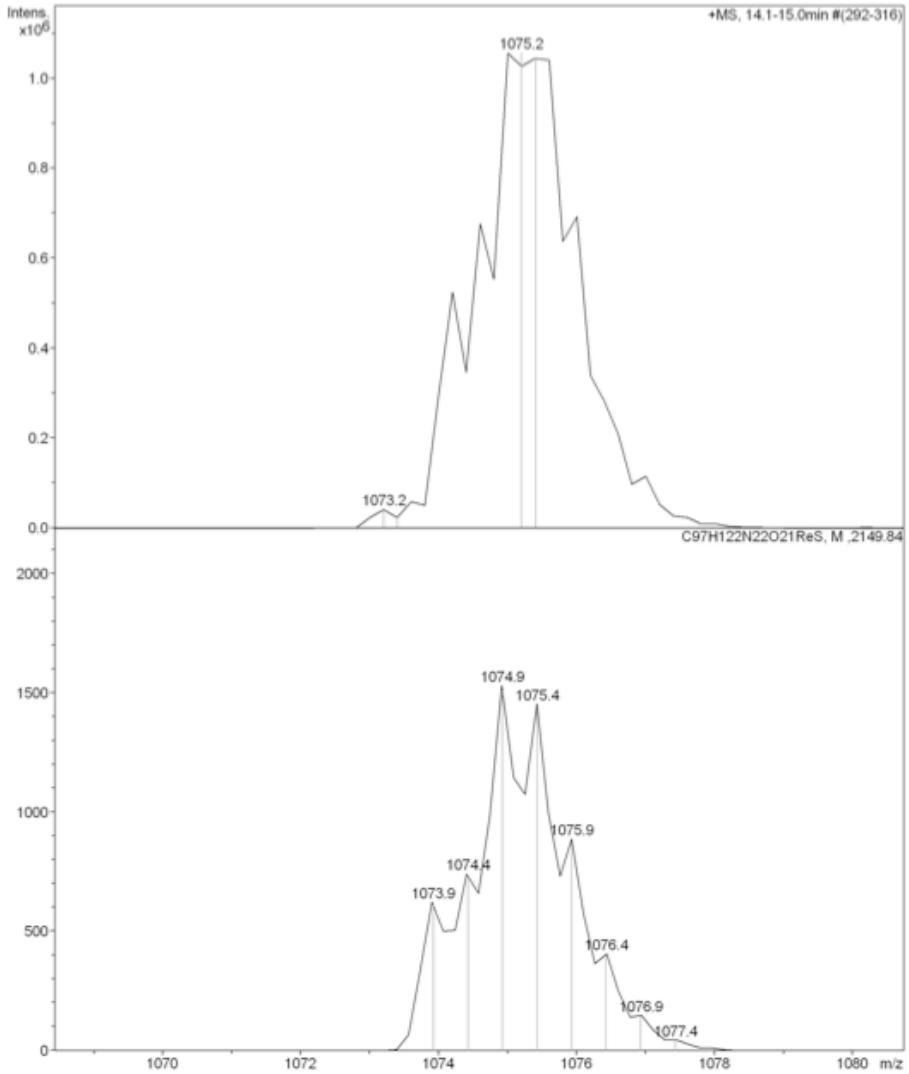

Figure S15. Recordered (above) and simulated (below) isotopic pattern of **Re-PLPG-Bombesin**.

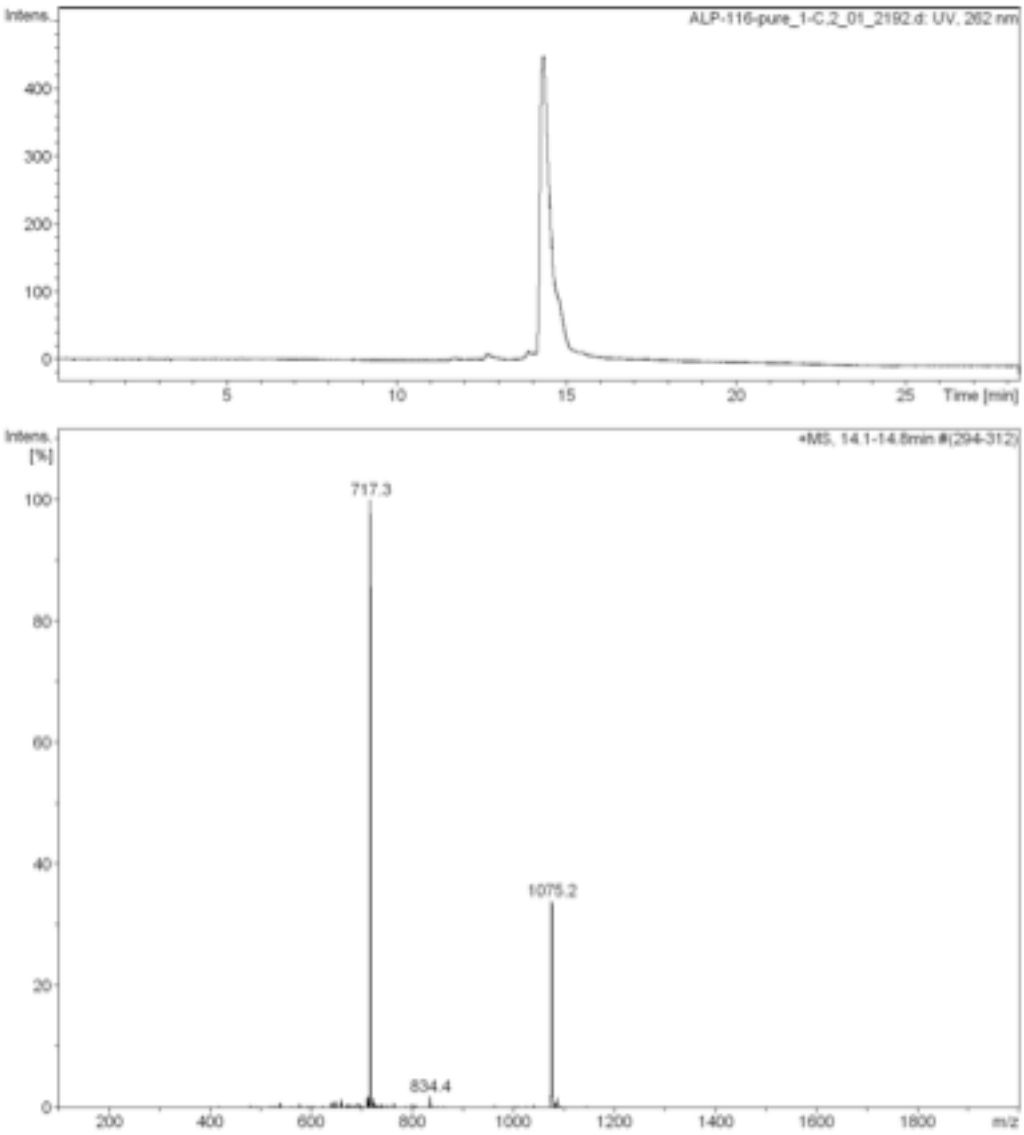

Figure S16. LC-MS spectrum of **Re-PLPG-Bombesin**.

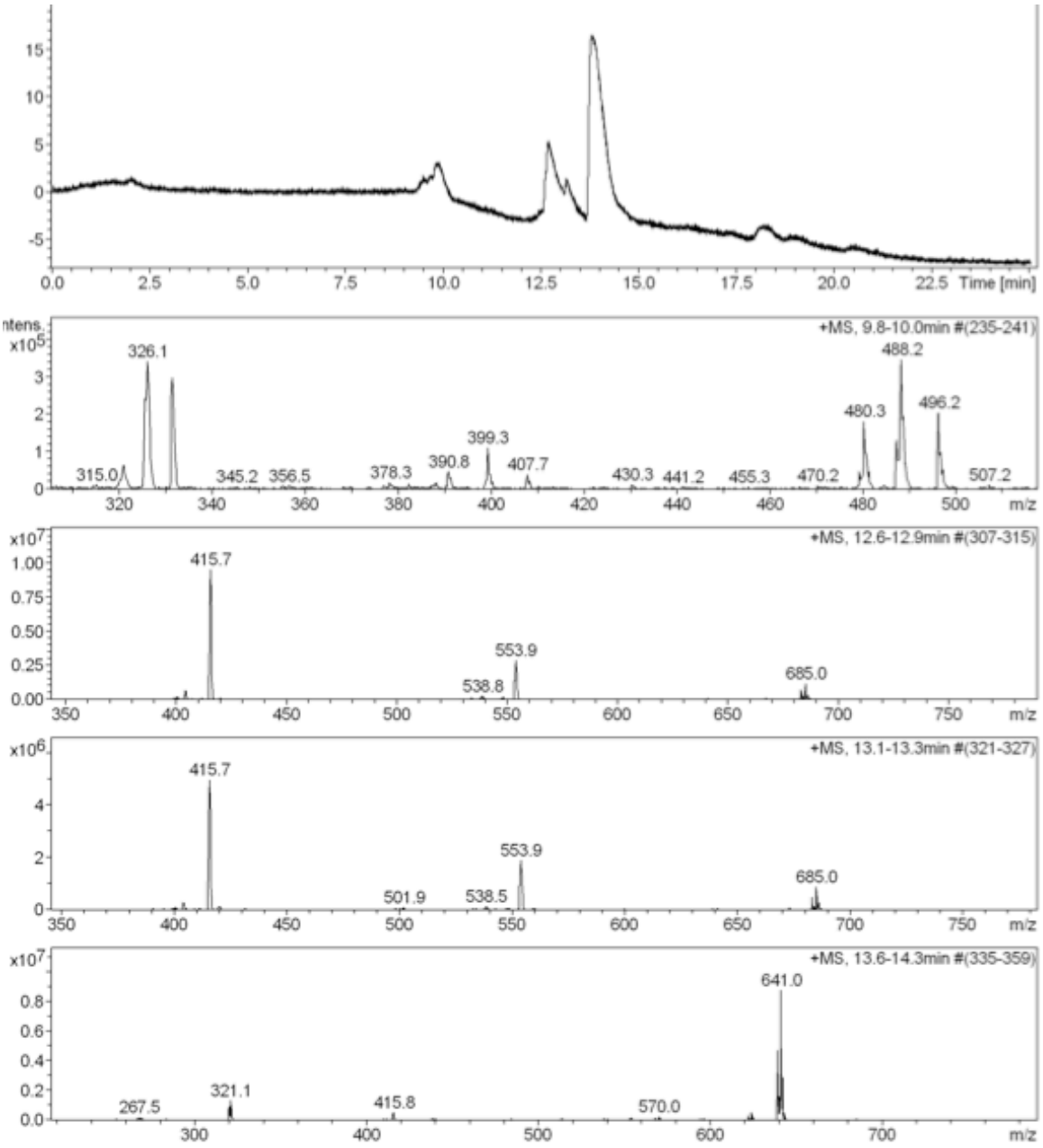

Figure S17. Photolysis of **Re-PLPG-NLS** followed by LC-MS.

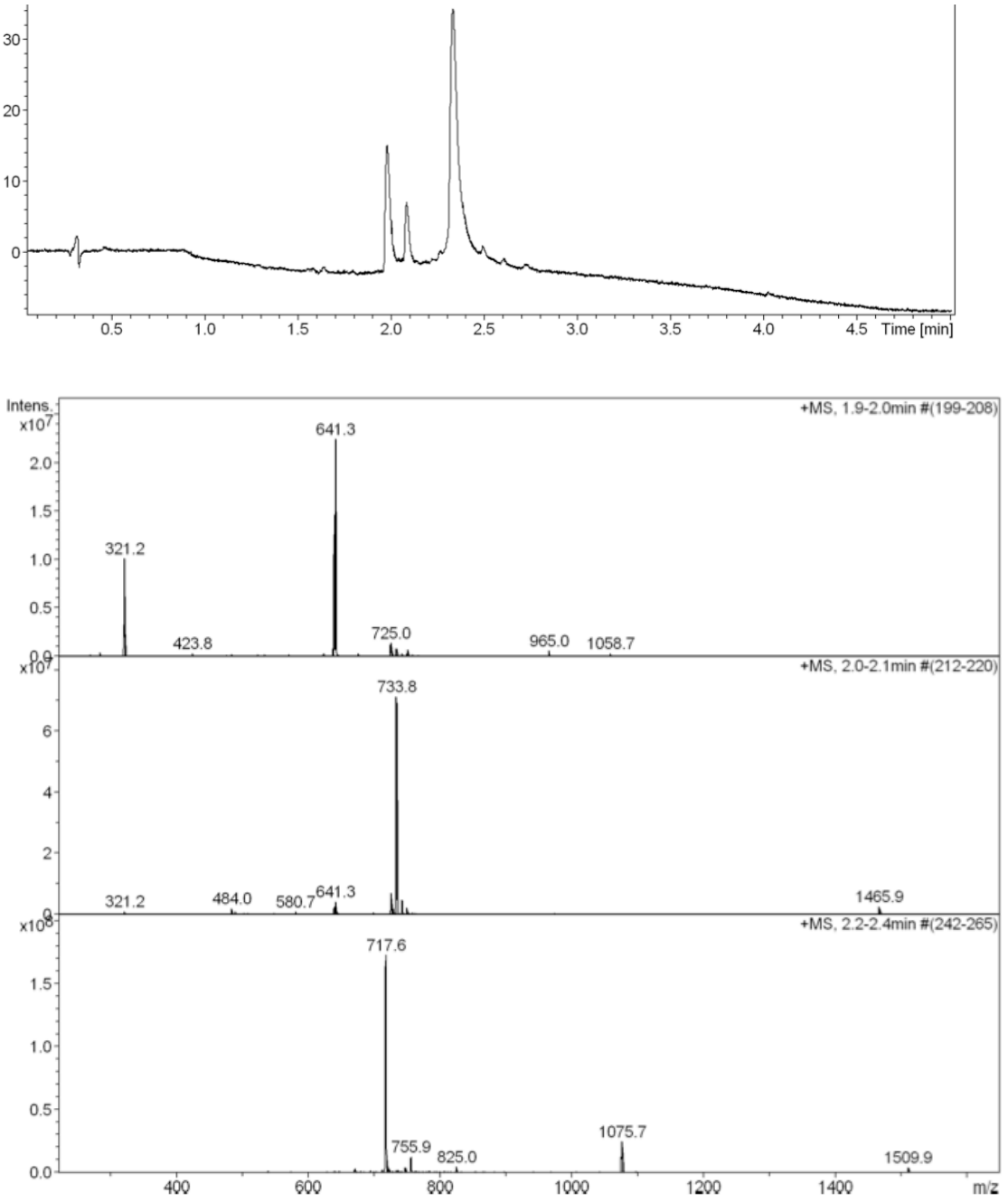

Figure S18. Photolysis of **Re-PLPG-Bombesin** followed by LC-MS.

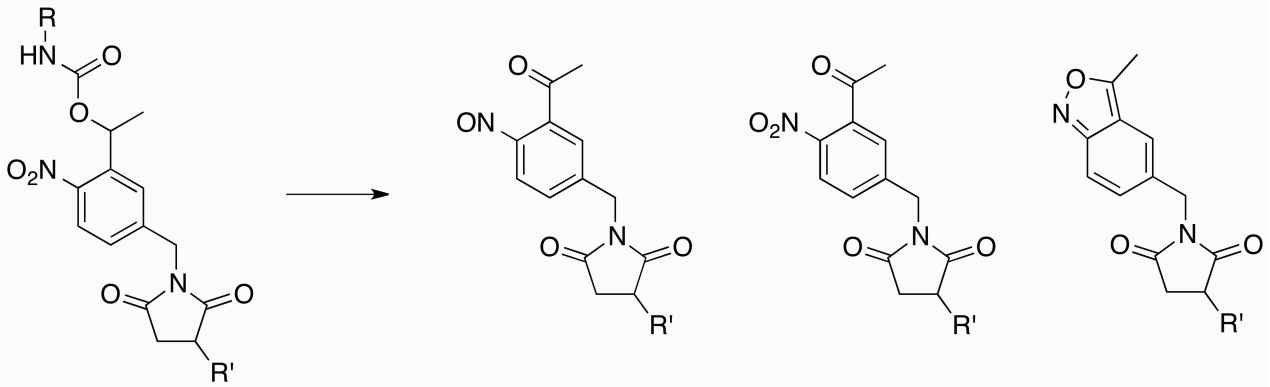

Figure S19. UVA-induced decomposition of PLPG and its products.

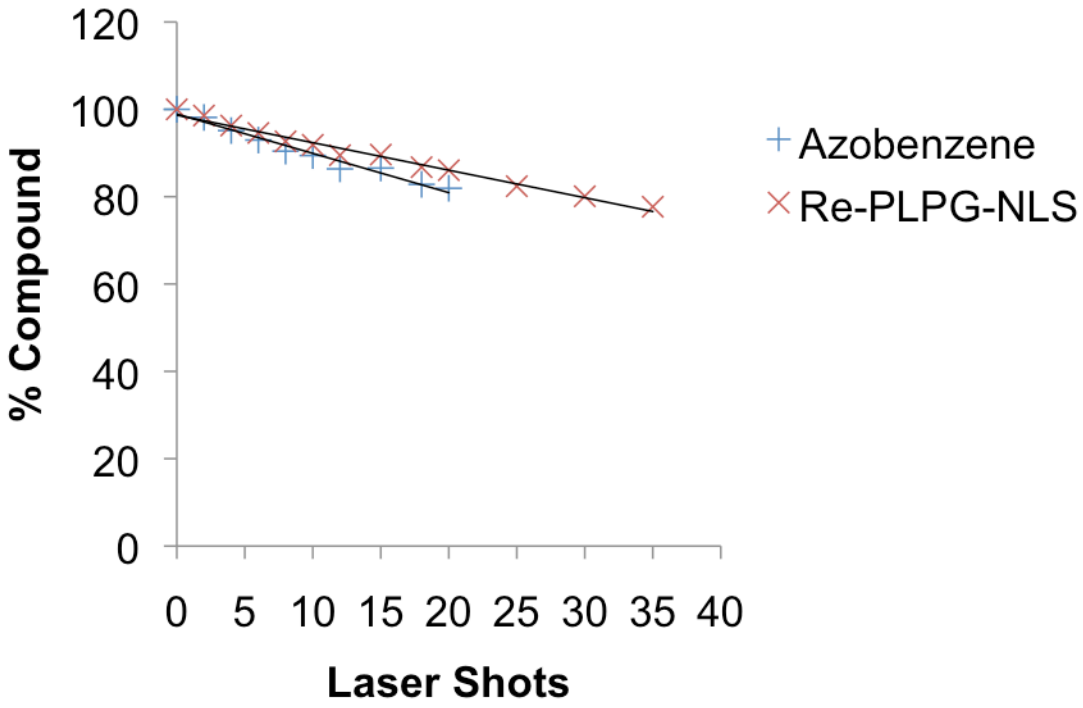

Figure S20. Laser photolysis of **Re-PLPG-NLS.**

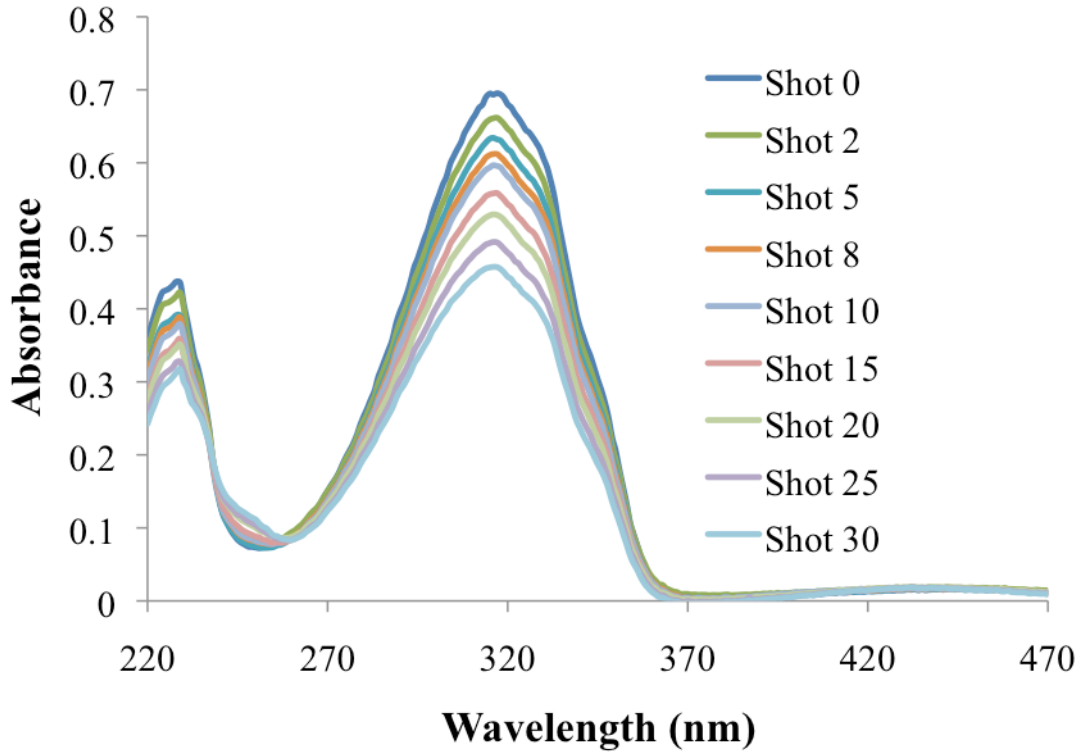

Figure S21. Photo-conversion of trans-azobenzene to cis-azobenzene followed by UV/vis.

Table S1: Singlet oxygen generation quantum yields.

Compound	Water	Acetonitrile
Re-NH_2	24%[a], 26%[b]	77%[a], 75%[b]
Re-NLS	23%[a], 26%[b]	79%[a], 76%[b]
Re-PLPG-NLS	24%[a], 25%[b]	75%[a], 76%[b]
Re-Bombesin	25%[b]	73%[b]
Re-PLPG-Bombesin	27%[b]	75%[b]

[a] measured by RNO/histidine assay (can not be used on bombesin derivatives, as bombesin sequence contains histidine); [b] measured by near-IR luminescence.

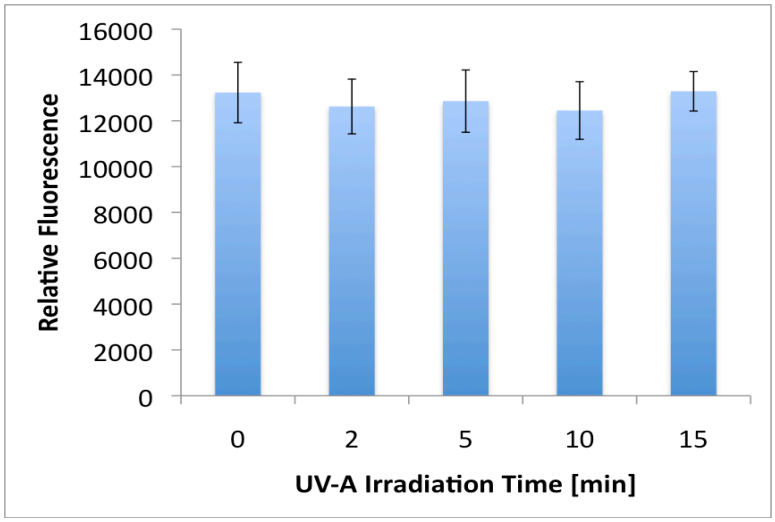

Figure S22. Resazurin assay determining the viability of MRC-5 cells irradiated with UVA (350 nm, 42 W/m^2).

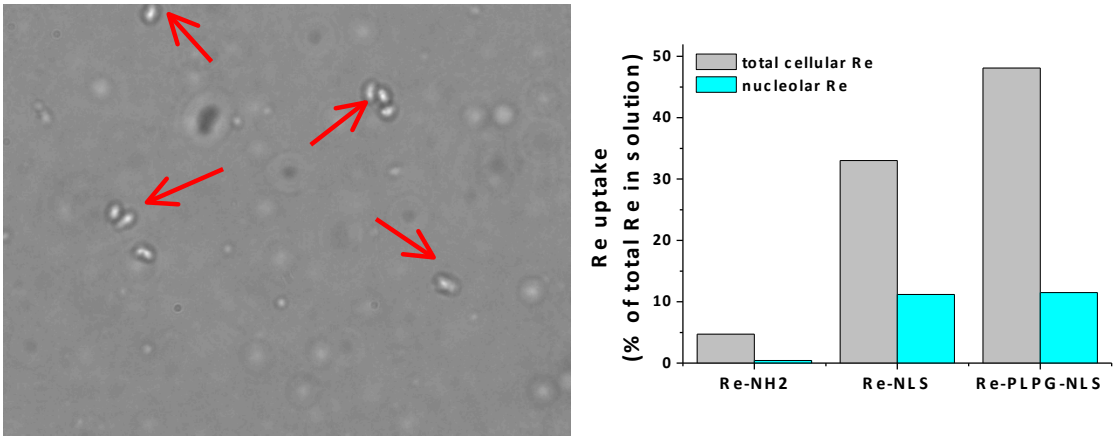

Figure S23. Left panel: phase contrast image of nucleoli isolated from HeLa cells; Right panel: uptake in HeLa cells treated with 20 µM of complex **Re-NH$_2$**, **Re-NLS** or **Re-PLPG-NLS** for 2 h, in whole cell extract and in nucleoli, determined by ICP-MS.

Figure S24. Electrophoretic resolution of pcDNA3 on 0.8% agarose gel upon treatment at different incubation temperature and in presence of BstXI (left) or treated with **NLS** at increasing concentration (right).

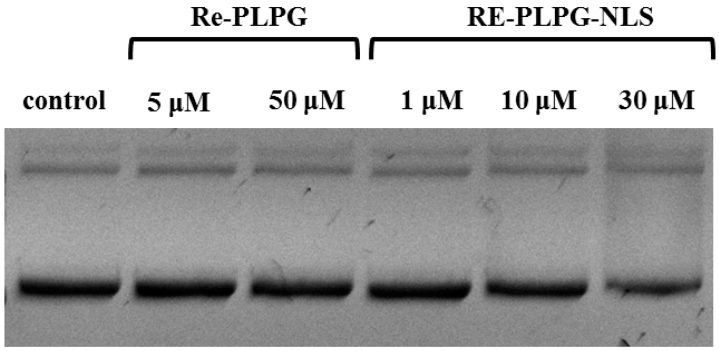

Figure S25. Electrophoretic resolution of pcDNA3 on 0.8% agarose gel upon treatment for 20 minutes at increasing concentration of RE-PLPG or Re-PLPG-NLS in the dark.

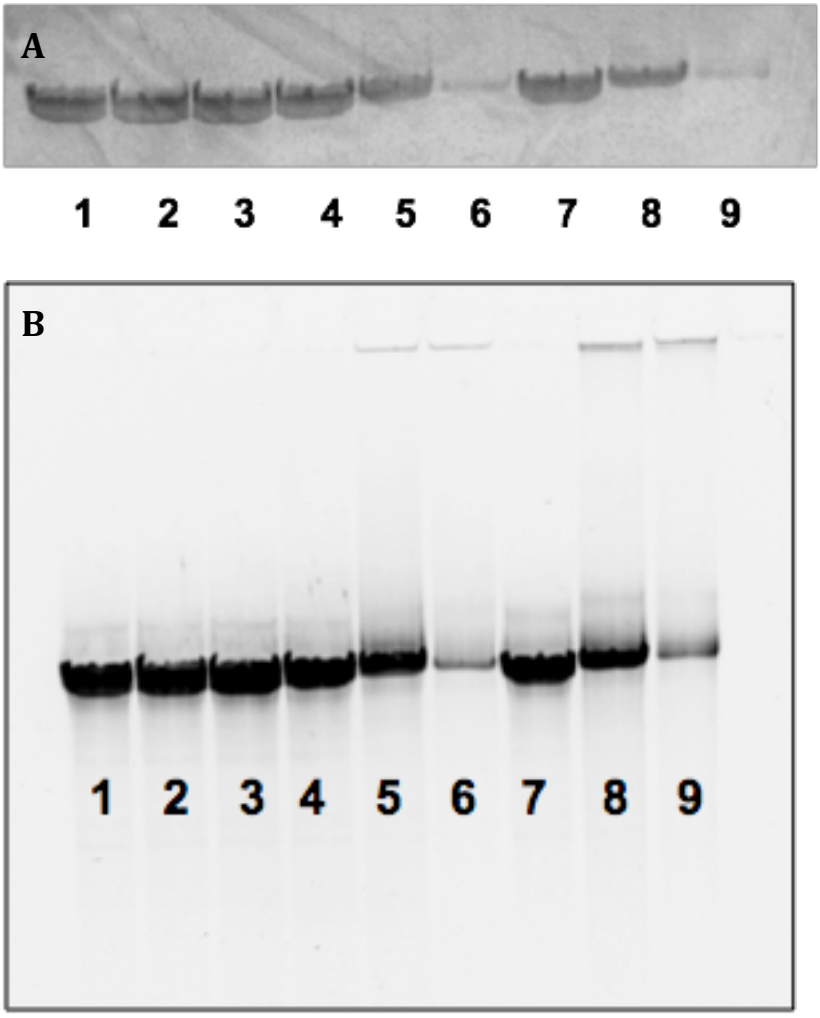

Figure S26. Denaturing polyacrylamide gel electrophoresis of D135-L14 ribozyme sequence from *Sc.*ai5*γ* intron of *S. cerevisiae* visualized by UV shading (A) and ethidium bromide (B). 1) RNA, 2) RNA irradiated for 5 min with UVA, 3) RNA incubated at r.t. for 30 min, 4-6) RNA incubated with 10, 50 or 100 μM of **Re-PLPG-NLS** for 30 min at r.t., 7-9) RNA incubated with 10, 50 or 100 μM of **Re-PLPG-NLS** for 30 min at r.t. and irradiated for 5 min with UVA.

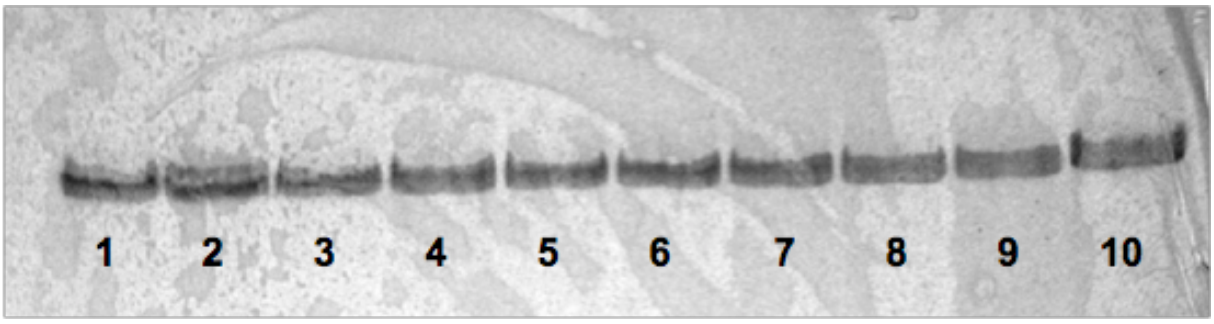

Figure S27. Denaturing polyacrylamide gel electrophoresis of D135-L14 ribozyme sequence from *Sc*.ai5*γ* intron of *S. cerevisiae* visualized by UV shading 1) and 10) RNA, 2) RNA irradiated for 5 min with UVA, 3) RNA incubated at r.t. for 30 min, 4-6) RNA incubated with 10, 50 or 100 μM of **Re-PLPG** for 30 min at r.t., 7-9) RNA incubated with 10, 50 and 100 μM of **Re-PLPG** for 30 min at r.t. and irradiated for 5 min with UVA.

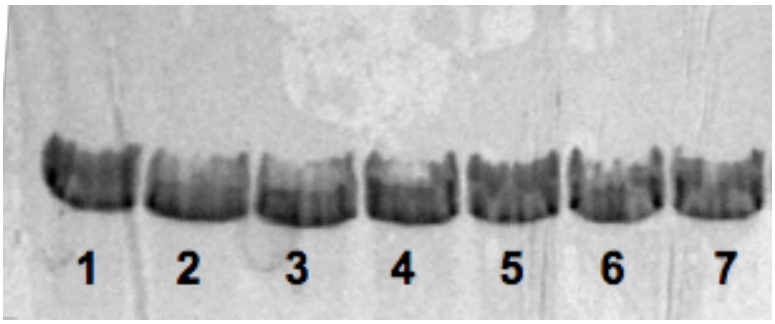

Figure S28. Denaturing polyacrylamide gel electrophoresis of D135-L14 ribozyme sequence from *Sc*.ai5*γ* intron of *S. cerevisiae* visualized by UV shading 1) RNA, 2) RNA irradiated, 3) RNA incubated at r.t. for 30 min, 4) and 5) RNA incubated with 10 or 100 μM of **Re-NH_2** for 30 min at r.t., 6) and 7) RNA incubated with 10 or 100 μM of **Re-NH_2** for 30 min at r.t. and irradiated for 5 min with UVA.

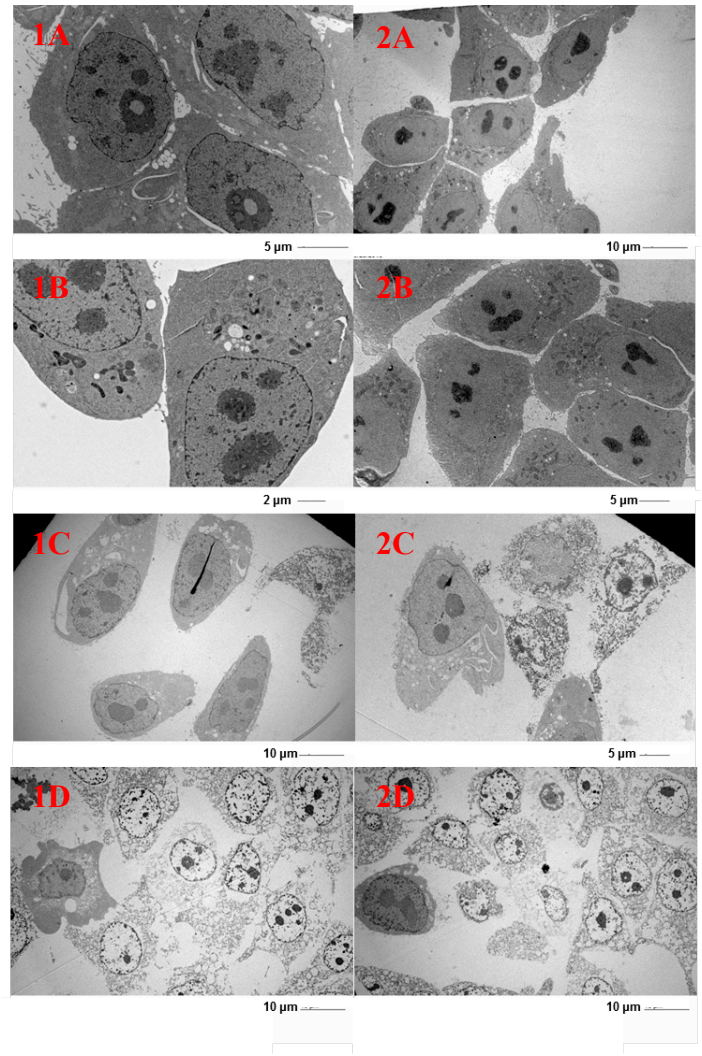

Figure S29. Cellular morphology study of HeLa cells treated for 2 h with 20 µM **Re-PLPG-NLS**; 1-2A) untreated cells (dark control); 1-2B) untreated cells (control irradiated at 350 nm for 10 minutes); 1-2C) HeLa cells treated with **Re-PLPG-NLS** in the dark; 1-2D) HeLa cells treated with **Re-PLPG-NLS** and irradiated at 350 nm for 10 minutes.

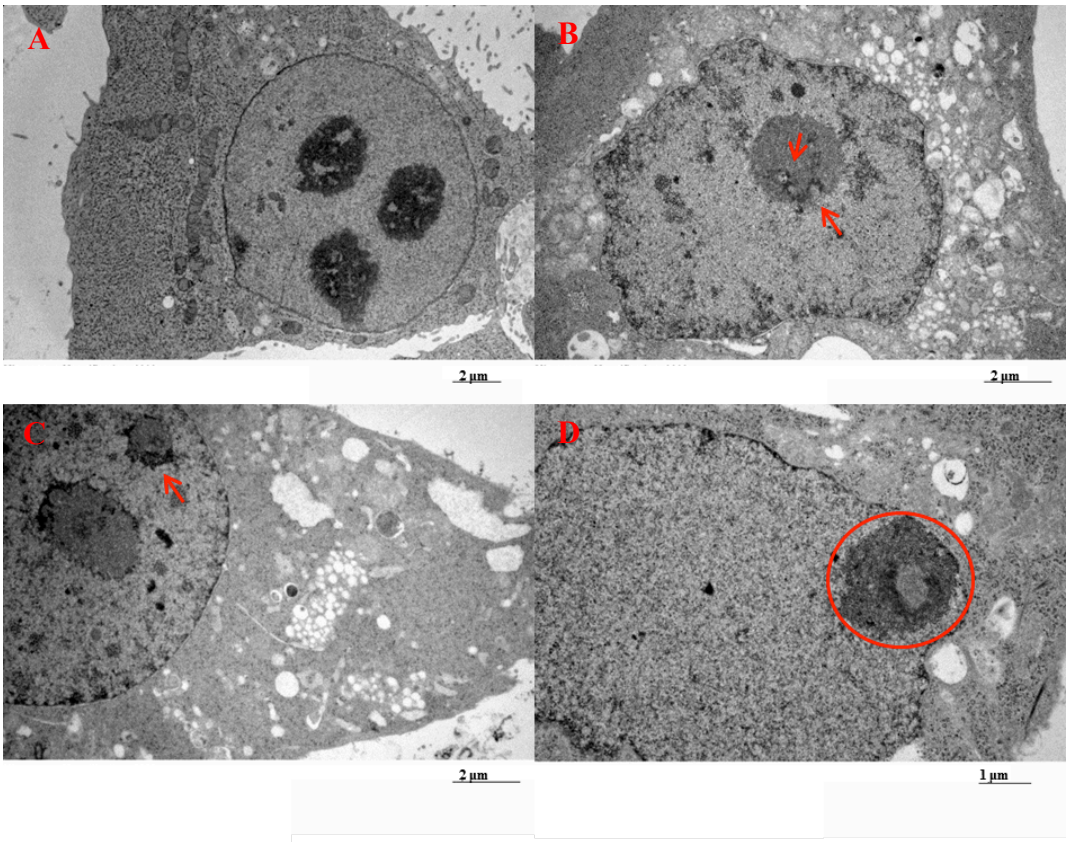

Figure S30. Nucleolar morphology study of HeLa cells treated for 2 h with 20 µM **Re-PLPG-NLS** and irradiated for 10 minutes at 350 nm; A) nucleolar component in the control; B) formation of nuclear caps around the nucleolar remnant; C) separation of fibrillar and granular center, migration and unraveling of fibrillar center at the peripheral part of the nucleolar body; D) migration of the whole nucleolar body to the peripheral part of the nucleus.

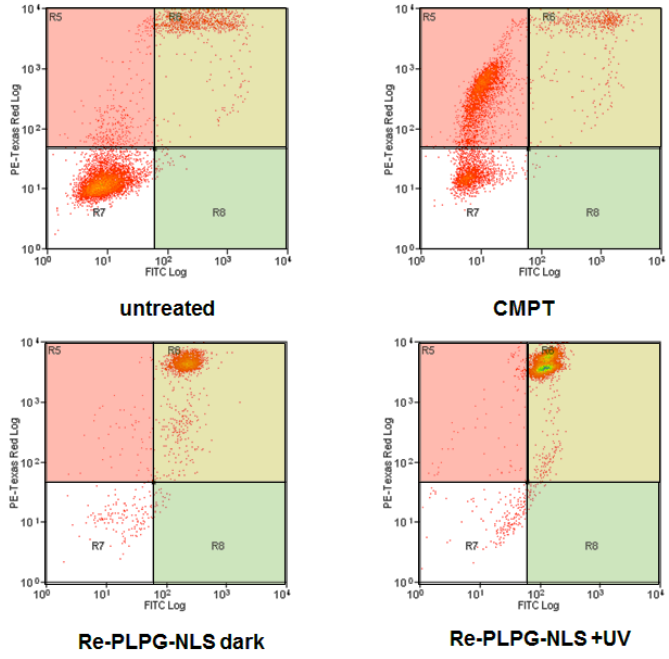

Figure S31. HeLa cells treated with 20 μM **Re-PLPG-NLS** and irradiated at 350 nm for 10 minutes, analyzed by flow cytometry with the Annexin V / PI staining; white/channel R7: viable cells, Annexin V negative, PI negative; green/channel R8: early apoptotic cells, Annexin V positive, PI negative; dark yellow/channel R6: late apoptotic cells, Annexin V positive, PI positive; red/channel R5: necrotic cells, Annexin V negative, PI positive.